Syntheses, Structures and Anticancer Activities of Two Tri(*o*-halobenzyl)tin Substituted Benzoates①

TAN Xu-Liang ZHANG Fu-Xing② HE Li-Fang
GUI Shi-Yin ZHANG Yi-Ling ZHU Xiao-Ming
SHENG Liang-Bing FENG Yong-Lan
YU Jiang-Xi JIANG Wu-Jiu

(*Department of Chemistry and Materials Science*, *Hengyang Normal University*; *Key Laboratory of Functional Metal-organic Complexes of Hunan Province*; *Key Laboratory of Functional Organometallic Materials of Colleges of Hunan Province*; *Hengyang*, *Hunan* 421008, *China*)

ABSTRACT Tri(*o*-chlorobenzyl)tin 2,4,6-trimethylbenzoate (**1**) and tri(*o*-bromobenzyl)tin salicylate (**2**) were synthesized and characterized by elemental analysis, IR spectroscopy, NMR (^{1}H, ^{13}C and ^{119}Sn), thermogravimetric analysis, and single-crystal X-ray diffraction. The *initio* calculation and in *vitro* anticancer activity test were performed for compounds **1** and **2**. They are both single tin nucleus structures and the tin atoms were tetracoordinated in a distorted tetrahedral configuration; Compounds **1** and **2** showed stronger anticancer activity than cisplatin in human cervical cancer cells (Hela), liver cancer cells (HuH-7), non-small cell lung cancer cells (A549), lung adenocarcinoma cells (H1975) and breast cancer (MCF-7).

Keywords: tri(*o*-chlorobenzyl)tin 2,4,6-trimethylbenzoate, tri(*o*-bromobenzyl)tin salicylate, crystal structure, quantum chemistry, in *vitro* antitumor activity; DOI: 10.14102/j.cnki.0254–5861.2011–3080

1 INTRODUCTION

Cancer has become a major killer threatening the human health, and the latest national cancer statistics released by the National Cancer Center cancer patients in China show that it accounts for more than 20% of the total number of patients in the world. In the past 10 years, the incidence of malignant tumors has increased by 3.9% annually, the mortality rate has increased by 2.5% annually, and the death rate from malignant tumors has accounted for 23.9% of all death in the country[1]. Drug therapy has become one of the important means for the clinical treatment of cancer. After years of continuous development, many important advances have been made in the research and development of anti-tumor drugs[2, 3]. However, faced with the solid tumor accounting for more than 90% of the malignant tumor at the most serious threat to human life and health, it is still so lack of efficient, specific drugs. Therefore, it is of great significance for the development of new anti-tumor drugs. Great interest has been aroused that the organotin compounds have inhibitory activity against the proliferation of cancer cells, which opens up a new direction for the development of highly selective, highly effective and low-toxicity anti-tumor drugs[4-6]. Studies have shown that many organotin complexes have extremely efficient and broad-spectrum anticancer activity, much higher than that of the anticancer drug cisplatin, which is widely used in clinical practice at present[7-12]. In addition, substituted aromatic carboxylic acids are a kind of ligands with rich structure and excellent properties, which can form organotin complexes with different structural characteristics and unique properties with alkyl tin. In recent years, some related studies have been carried out on this kind of organotin complexes[13-16]. To continue the systematic research, tri(*o*-chlorobenzyl)tin 2,4,6-trimethylbenzoate (**1**) and tri(*o*-bromobenzyl)tin salicylate (**2**) have been synthesized, characterized by elemental analysis, infrared spectrum and nuclear magnetic

Received 25 December 2020; accepted 16 March 2021 (**CCDC 1938462, 1938463 and 1938464**)

① The project was supported by the open fund project of Hunan Provincial innovation platform (18K089), the key project of Hunan Provincial education department (19A070), the open fund of Hunan Provincial key laboratory (M018K07), Hengyang science and technology plan project, Hunan Provincial applied characteristic discipline fund, and Hunan Provincial science and technology innovation team support plan

② Corresponding author. Zhang Fu-Xing, Tel: 0734-8484932; E-mail: zfx8056@163.com

resonance (^{1}H, ^{13}C and ^{119}Sn), and X-ray single-crystal diffraction. The HOMO and LUMO molecular orbitals and composition characteristics of some frontier molecular orbitals were calculated and presented. Thermal stability and*in vitro* anticancer activity of **1** and **2** were also investigated.

2 EXPERIMENTAL

2. 1 Instruments and reagents

NCI-H460, HepG2 and MCF7 cells were obtained from the U.S. tissue culture library (ATCC). RPMI 1640 medium with 10% fetal bovine serum was purchased from GIBICO. Carboplatin was purchased from Qilu pharmaceutical technologies Co. LTD. The other reagents were analytically pure.

Italian MILESTONE microwave synthesizer was employed for the compounds. IR spectra were recorded using the Shimadzu Prestige 21 infrared spectrometer in the range of 4000 ～ 400 cm^{-1} (KBr pellets). Element analysis was performed by PE-2400 (II) element analyzer. ^{1}H, ^{13}C and ^{119}Sn NMR were measured by Bruker Avance III HD 500MHz NMR (TMS was selected as the internal standard). Melting point was measured by Beijing Tektronix X-4 binocular photomicrography (thermometer not corrected).

2. 2 Synthesis of the compounds

Compound 1 The methanol solution (30.0 mL) of tri(*o*-chlorobenzyl)tin (0.659 g, 1.0 mmol), 2,4,6-trimethylbenzoic acid (0.164 g, 1.0 mmol) and triethylamine (1.0 mmol) was added into the microwave reaction tank with microwave reaction for 2.0 h at 120 °C, then the mixture was cooled and filtered. After part of the solvent of filtrate was removed with rotary evaporation, the residue was placed and the white solid was found. Recrystallization with the mixed solvent of cyclohexane and dichloromethane afforded colorless crystals of **1** (yield 72.23%, 0.476 g). m.p.: 107～109 °C. Anal. Calcd. (%) for $C_{31}H_{29}Cl_3O_2Sn$: C, 56.52; H, 4.41. Found (%): C, 56.82; H, 4.36. FT-IR (KBr, cm^{-1}): 3051, 2974, 2932, 2872 ν(C–H), 1632 ν_{as}(COO$^-$), 1389 ν_s(COO$^-$), 590 ν(Sn–C), 453 ν(Sn–O). ^{1}H NMR ($CDCl_3$, 500 MHz) 7.28～7.23 (m, 4H), 7.09～7.06 (m, 3H), 7.02～6.99 (m, 5H), 6.83 (d, J = 4.0 Hz, 2H), 2.76 (s, 6H), 2.30 (s, 3H), 2.28 (s, 3H), 2.26 (s, 3H); ^{13}C NMR ($CDCl_3$, 125 MHz) δ 169.78, 139.41, 137.56, 135.27, 132.33, 130.45, 130.09, 129.67, 129.56, 128.84, 128.39, 126.98, 126.26, 25.53, 21.07, 20.18, 19.77. ^{119}Sn NMR ($CDCl_3$, 187 MHz, Me_4Sn) 1.93.

Compound 2 The preparation was the same as that for **1** except that tri(*o*-chlorobenzyl)tin was replaced by tri(*o*-bromobenzyl)tin (0.665 g, 1.0 mmol) and 2,4,6-trimethylbenzoic acid by salicylic acid (0.138 g, 1.0 mmol). Colorless crystals of **2** were obtained in 67.23% yield (0.515 g). m.p.: 120～122 °C. Anal. Calcd. (%) for $C_{28}H_{23}Br_3O_3Sn$: C, 43.91; H, 3.03. Found (%): C, 43.87; H, 3.01. FT-IR (KBr, cm^{-1}): 3439 ν(O–H), 3061, 3013, 2957, 2922, 2862 ν(C–H), 1726 ν_{as}(COO$^-$), 1474 ν_s(COO$^-$), 565 ν(Sn–C), 434 ν(Sn–O). ^{1}H NMR ($CDCl_3$, 500 MHz), δ(ppm): 11.36 (s, 1H), 7.72 (dd, J = 7.5 Hz, J = 1.0Hz, 1H), 7.50～7.44 (m, 3H), 7.42～7.38 (m, 1H), 7.15～7.12 (m, 3H), 7.07～7.03 (m, 3H), 6.96～6.93 (m, 4H), 6.84～6.81 (m, 1H), 2.90 (s, 6H). ^{13}C NMR ($CDCl_3$, 125 MHz), δ(ppm): 174.56, 161.51, 139.06, 134.79, 132.16, 131.31, 130.12, 127.65, 127.58, 126.62, 123.64, 118.58, 116.91, 29.29. ^{119}Sn NMR ($CDCl_3$, 186 MHz), δ(ppm): –12.13.

2. 3 Determination of the crystal structure

Suitable samples (0.26mm × 0.17mm × 0.13mm for **1** and 0.23mm × 0.21mm × 0.20mm for **2**) were chosen and mounted on the Bruker SMART APEX II CCD single crystal diffractometer with graphite-monochromated Mo-$K\alpha$ radiation (λ = 0.071073 nm) with a φ~ω scan mode at 296(2) K. All the data were corrected by *Lp* factors and empirical absorbance. The structure was solved by direct methods. All non-hydrogen atoms were determined in successive difference Fourier synthesis, and all hydrogen atoms were added according to theoretical models. All hydrogen and non-hydrogen atoms were refined by isotropic and anisotropic thermal parameters through full-matrix least-squares techniques. All calculations were completed by Wing and the SHELXTL-97 program. The selected bond lengths and bond angles for **1** and **2** are listed in Tables 1 and 2, respectively.

Table 1. Crystallographic Data of the Compounds

Compound	**1**	**2**
Empirical	$C_{31}H_{29}Cl_3O_2Sn$	$C_{28}H_{23}Br_3O_3Sn$
Formula weight	658.58	765.88
Crystal system	Monoclinic	Triclinic

To be continued

Space group	$P2_1/c$	$P\bar{1}$
a/nm	1.0920(1)	1.1230(1)
b/nm	1.3643(1)	1.1251(1)
c/nm	2.0213(1)	1.1300(1)
α/°	90	104.119(1)
β/°	96.517(1)	99.364(1)
γ/°	90	91.025(1)
V/nm^3	2.992(4)	1.3637(2)
Z	4	2
D_c (g·m^{-3})	1.462	1.865
μ(Mo$K\alpha$) (cm^{-1})	11.48	5.360
F(000)	1328	740
Crystal size/mm	0.26×0.17×0.13	0.23×0.21×0.20
Temperature/K	296(2)	296(2)
θ range for data collection	1.80≤θ≤25.05	2.40≤θ≤27.60
Index range	–12≤h≤13, –16≤k≤15, –24≤l≤16	–14≤h≤14, –14≤k≤14, –14≤l≤14
Reflections collected	14903	16957
Reflections collected/unique	5284 (R_{int} = 0.0188)	6240 (R_{int} = 0.0309)
Goodness-of-fit on F^2	1.063	1.038
Final R indices R, wR ($I > 2\sigma(I)$)	0.0460, 0.1363	0.0369, 0.0751
R indices (all data)	0. 0548, 0.1446	0.0615, 0.0823
Largest diff. peak and hole (e·nm^{-3})	1721 and –968	1436 and –548

Table 2. Parts of Bond Lengths (nm) and Bond Angles (°) of the Compounds

1					
Bond	Dist.	Bond	Dist.	Bond	Dist.
Sn(1)–O(1)	0.2063(4)	Sn(1)–C(11)	0.2152(6)	Sn(1)–C(18)	0.2157(5)
Sn(1)–C(25)	0.2159(5)				
Angle	(°)	Angle	(°)	Angle	(°)
O(1)–Sn(1)–C(11)	109.8(2)	O(1)–Sn(1)–C(18)	95.47(18)	C(11)–Sn(1)–C(18)	115.0(2)
O(1)–Sn(1)–C(25)	106.59(18)	C(11)–Sn(1)–C(25)	111.7(2)	C(18)–Sn(1)–C(25)	116.5(2)
2					
Bond	Dist.	Bond	Dist.	Bond	Dist.
Sn(1)–O(1)	0.2081(3)	Sn(1)–C(15)	0.2143(4)	Sn(1)–C(8)	0.2149(4)
Sn(1)–C(1)	0.2155(4)				
Angle	(°)	Angle	(°)	Angle	(°)
O(1)–Sn(1)–C(15)	105.65(13)	O(1)–Sn(1)–C(8)	109.39(14)	C(15)–Sn(1)–C(8)	112.22(15)
O(1)–Sn(1)–C(1)	96.06(13)	C(15)–Sn(1)–C(1)	116.82(16)	C(8)–Sn(1)–C(1)	114.76(15)

2. 4 Anticancer activity studies

The drug was dissolved in a small amount of DMSO. Then the mixture was diluted with water to the required concentration, and maintained the final concentration of DMSO < 0.1%. NCI-H460, HepG2 and MCF7 cells were cultured in vitro using RPMI 1640 (GIBICO) culture medium containing 10% fetal bovine serum in a 5% (volume fraction) CO_2, 37 °C saturated humidity incubator. In vitro anti-cancer drug sensitivity test was determined by MTT assay. The number of experimental cells was adjusted to obtain the absorbance of 1.3~2.2 at 570 nm, the test solution of the compounds (0.1 nmol·L^{-1}~10 μmol·L^{-1}) was set 6 concentrations, the cells were treated for 72 h, and each concentration was tested at least 3 parallel and 3 repeated experiments. IC_{50} was obtained with GraphPad Prism version 5.0 programs.

3 RESULTS AND DISCUSSION

3. 1 Spectral analyses

In the infrared spectra, the absorption peaks of **1** and **2** appeared at 453 and 434 cm^{-1}, respectively, indicating the formation of Sn–O bond. The values of Δv between v_{as} and v_s carboxylate groups ($\Delta v = v_{as} - v_s$) are 250 and 243 cm^{-1}, more than 200 cm^{-1}, indicating the presence of monodentate coordination mode of the carboxylate groups. In compound **2**, a broad strong absorption peak at 3439 cm^{-1} is the characteristic stretching vibration of the phenolic hydroxyl group, suggesting the phenolic hydroxyl group does not

participate in coordination.

In the ^{1}H NMR spectrum, the absorption peak of **2** with a single phenolic hydroxyl group appeared at 11.36, suggesting the existence of free phenolic hydroxyl group, which was consistent with the result of infrared spectrum. The multiple peaks (7.28~6.83 for **1** and 7.72~6.81 for **2**) belong to the proton absorption peaks of aromatic ring. The absorption peaks of methylene hydrogen associated with tin locate at 2.28 (**1**) and 2.90 (**2**), respectively. Interestingly, the absorption peaks of the three methyl groups on the benzene ring of **1** appear at 2.30, 2.28 and 2.26 correspondingly, which may be attributed to the inconsistent chemical environment of the three methyl groups due to their spatial effects. The ratio of peak area and the number of protons in each group is basically the same.

In ^{13}C NMR spectra, the absorption peaks of carbonyl and methylene carbon of **1** and **2** are observed at 169.78 and 174.56, 25.53 and 29.29, respectively. The absorption peaks of aromatic ring carbon appear at 139.41~126.26 and 161.51~116.91. In **2**, the absorption peaks is found at low field (161.51) due to the electron-pulling effect of phenolic hydroxyl group on the adjacent carbon. The absorption peaks of the three methyl carbon atoms on the benzene ring of **1** are 21.07, 20.18 and 19.77, respectively.

In ^{119}Sn NMR spectra, the absorption peaks of **1** and **2** appeared respectively at 1.93 and –12.13.

Furthermore, the aforesaid analysis conformed to the crystal test results.

3. 2 Structure description

As shown in Figs. 1 and 2 and Table 2, both compounds demonstrate a single nuclear structure, where the Sn atom center is four-coordinated by three methylene C atoms and one carboxyl O atom to form a tetrahedral configuration. The bond lengths and bond angles of Sn–C are not equal due to the base space interaction between the ligand and Cl (Br) atom. The distances between Sn(1) and O(1) in **1** and **2** are 0.2063 and 0.2081 nm, respectively, indicating that Sn(1) is well bonded with O(1). However, the distances of Sn(1) and O(2) with 0.2855 nm (**1**) and 0.2867 nm (**2**) are longer than the sum of the two atomic covalent radii (0.216 nm), suggesting that Sn(1) and O(2) can not bond with each other. As a result, the Sn atom center adopts a four-coordinated distorted tetrahedral configuration with a monodentate coordination mode of the carboxylate groups, which is consistent with the results of IR spectra.

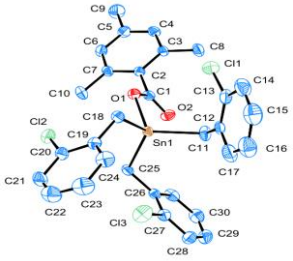

Fig. 1. Molecular structure of 1 with the ellipsoids drawn at 20% probability level

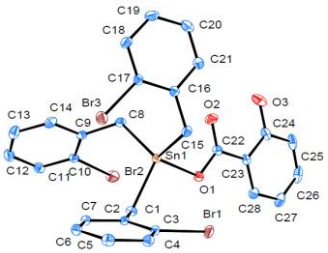

Fig. 2. Molecular structure of 2 with the ellipsoids drawn at the 20% probability level

3. 3 Orbital analysis

According to the atomic coordinates of the crystal structure, the total energy of the molecule and the energy of the frontier molecular orbital were calculated by the Gaussian 03W program at the B3lyp/lanl2dz basis group level.

Compound **1**: E_T = –1396.7001335 a.u., E_{HOMO} = –0.26452 a.u., E_{LUMO} = 0.23005 a.u. and $\Delta E_{LUMO\text{-}HOMO}$ = 0.49457 a.u.. Compound **2**: E_T = –1348.7418491 a.u., E_{HOMO} = –0.23332 a.u, E_{LUMO} = 0.04993 a.u. and $\Delta E_{LUMO\text{-}HOMO}$ = 0.18339 a.u. For the energy gap (ΔE) value between the lowest and highest occupied orbitals, both compounds have significant values, so they are more difficult to lose electron to be oxidized from the perspective of redox transfer. Furthermore, **2** has smaller ΔE value than **1**, showing it is more likely to lose electrons to be oxidized. Therefore, **1** has better stability than **2**.

In order to explore the electronic structure and bonding characteristics of both compounds, the molecular orbitals of **1** and **2** were analyzed, and the contribution of these orbitals in molecular orbitals was represented by the sum of the squares of the coefficients of atomic orbitals, which were normalized. The atoms of compounds were divided into seven parts. For **1**: (a) Sn atom; (b) methylene carbon C(1); (c) carbon atom of ligand carboxyl and oxygen atom L; (d) C(2) atom of *o*-chlorobenzyl benzene ring; (e) carbon atom C(3) of ligand trimethylphenyl; (f) Cl atom; (g) H atom. For **2**: (a) Sn atom; (b) methylene carbon C(1); (c) carbon atom of ligand

carboxyl and oxygen atom L; (d) C(2) atom of *o*-bromophenyl benzene ring; (e) hydroxyl oxygen atom of ligand and benzene ring carbon atoms M; (f) Br atom; (g) H atom. Five frontier occupied and unoccupied orbitals are taken respectively, and the calculated results are shown in Tables 3 and 4 as well as Figs. 3 and 4.

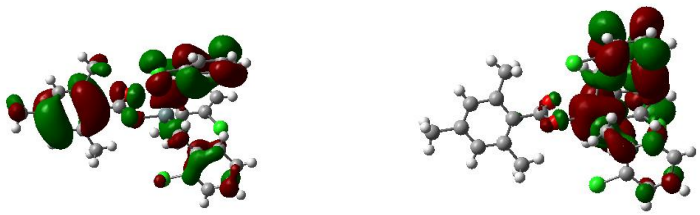

HOMO LUMO

Fig. 3. Schematic diagram of the frontier MO for 1

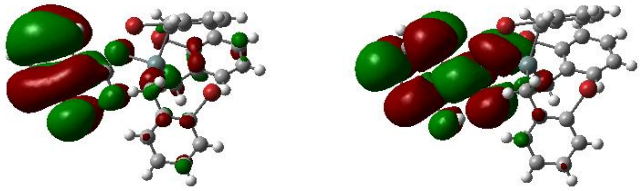

HOMO LUMO

Fig. 4. Schematic diagram of the frontier MO for 2

Table 3. Some Calculated Frontier Molecular Orbitals Composition of 1

	ε/Hartree	Sn	C1	L	C2	C3	Cl	H
162	–0.28336	3.62990	3.32456	6.02300	69.54044	1.17901	15.50466	0.79117
163	0.27705	6.72870	10.93509	2.35095	63.41439	3.75553	10.92781	1.88764
164	–0.27108	0.14667	0.24031	1.12485	0.83604	93.50925	0.15456	3.97704
165	–0.26542	0.97257	1.19043	7.90160	5.62748	79.97646	1.13979	3.18615
166HO	–0.26452	6.19268	9.88294	4.35567	61.74021	4.22176	11.72096	1.88567
167LU	0.23005	0.32553	0.12113	0.03937	97.25438	0.02196	2.19759	0.03634
168	0.23140	2.62849	0.44386	0.45290	95.72641	0.14546	0.37226	0.22757
169	0.23333	0.78516	0.25392	0.01815	97.29464	0.01211	1.53028	0.09522
170	0.23953	9.07432	2.18697	0.69406	85.22180	0.07579	2.06230	0.68343
171	0.24789	7.25408	1.40921	0.95038	86.40939	1.40422	1.59512	0.97390

As shown in Table 3 and Fig. 3, among the frontier-occupied molecular orbitals, the most contributions to molecular orbitals are carbon and chlorine atoms of *o*-chloro-benzyl benzene ring with 79.98% and 11.72%, respectively, indicating that the chlorobenzyl ring has strong stability. Secondly, the contribution rate of methylene carbon atom, Sn atom and carboxyl group (C and O) are 9.88%, 6.19% and 4.36%, respectively, confirming that the Sn–C and Sn–O bonds in the molecule are stable, and **1** has good stability. By comparing the components of atomic orbitals of HOMO and LUMO, the electrons are excited from HOMO to LUMO, and those on other atoms are concentrated to the benzene ring of *o*-chlorophenyl group, which is the only acceptor of electron transfer.

Table 4 and Fig. 4 show the bond characteristics of **2**. Among the frontier-occupied molecular orbitals, the most contributions to molecular orbitals are carbon and oxygen atoms of *o*-hydroxyphenyl benzene ring with 90.91%, indicating good conjugation and stability of the *o*-hydroxy-phenyl group. The contributions of Sn atom, methylene carbon atom and carboxyl group (C and O) atom are 2.63%, 2.32% and 2.19%, respectively, which suggested that Sn–C and Sn–O bonds have certain strength and **2** is stable in the ground state. By comparing the components of atomic orbitals of HOMO and LUMO, it can be seen that when electrons are excited from HOMO to LUMO orbital, it is mainly the electrons on the *o*-hydroxyphenyl group that transfer to other atoms through the carboxyl group. Carboxyl groups serve as both the bridge and the main acceptor of electron transfer.

Table 4. Some Calculated Frontier Molecular Orbitals Composition of 2

	ε/Hartree	Sn	C1	L	C2	M	Br	H
116	–0.25456	1.05659	4.37626	0.28937	73.70814	0.19735	19.96855	0.39027
117	–0.25076	2.86405	0.70141	1.20381	63.36991	0.45229	30.83806	0.52465
118	–0.24054	4.40320	17.35048	1.27756	59.00171	2.97421	13.11899	1.83861
119	–0.23808	4.63419	19.19896	0.84630	60.24315	0.40922	13.10924	1.12969
120HO	–0.23332	2.62339	2.32479	2.18871	1.58922	90.90507	0.27627	0.08313
121LU	–0.04993	4.86770	3.54722	34.28758	4.85518	51.66378	0.15642	0.59336
122	–0.02593	29.75247	8.20768	2.80554	55.23722	1.19942	2.15581	0.54029
123	–0.01827	1.99171	1.77308	0.90632	90.47927	0.68656	2.37397	1.34240
124	–0.01597	1.43215	2.03819	0.45223	91.68250	0.32729	2.23004	1.72883
125	–0.01377	1.52391	1.75692	0.34706	93.45448	0.44327	1.76048	0.38653

3. 4 Thermal stability analysis

Thermogravimetric tests were performed on the TG209F3 thermal analyzer under 20 mL/min flowing air, when ramping the temperature from 40 to 800 ℃ at a rate of 20 ℃/min. As shown in Fig. 5, compounds **1** and **2** are respectively thermally stable up to 150 °C and under 130 ℃, corresponding to the orbital analysis result. In **1**, there is a rapid weight loss between 180 and 290 °C, and weight loss basically stops at 700 ℃ of 76.91%. The residue can be assumed to be SnO_2, which is in agreement with the calculated value of 22.88%. In **2**, the weight loses rapidly from 165 to 340 °C, then gradually slows down until 610 ℃, with the residue assumed to be SnO_2 (17.69%), which is basically consistent with the calculated value of 19.68%.

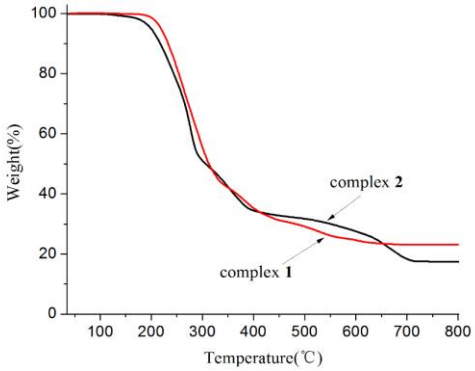

Fig. 5. Thermogravimetric analysis curves of the compounds

3. 5 Anticancer activity

Compared with cisplatin, the growth inhibitory activity of the compounds against tumor cells human cervical cancer cells (Hela), liver cancer cells (HuH-7), human non-small cell lung cancer cells (A549), lung adenocarcinoma cells (H1975), breast cancer cells (MCF-7) and normal human renal epithelial cells (293T) was tested in vitro, and the results are shown in Table 5. Compound **1** shows much stronger inhibitory activity than cisplatin against the tested tumor cells except MCF-7, and **2** exhibits relatively stronger inhibitory activity than **1**, but both compounds have weaker inhibitory activity against 293T than cisplatin.

Table 5. IC_{50} of Complexes and Cisplatin on Tumor Cells in Vitro (μmol·L^{-1})

	Hela	HuH-7	A549	H1975	MCF-7	293T
1	1.454 ± 0.356	0.482 ± 0.050	1.808 ± 0.432	1.166 ± 0.053	0.781 ± 0.224	2.255 ± 0.312
2	0.561 ± 0.266	0.101 ± 0.062	0.710 ± 0.271	0.359 ± 0.166	0.286 ± 0.100	0.918 ± 0.006
Cisplatin	57.025 ± 8.805	3.608 ± 1.099	2.439±0.829	16.803 ± 9.598	0.301 ± 0.147	33.245 ± 4.175

As we know, only two compounds with similar structure of **2**, tri(*o*-bromobenzyl)tin dithiotetrahydropyrrolocarbamate[17] and di(*p*-chlorobenzy)tin salicylate[18], have been carried out inhibitory activity test against MCF-7. The results manifested their IC_{50} to be 28.42 and 0.90 mol·L^{-1}, respectively. Compound **2** has stronger inhibitory activity with IC_{50} of 0.286 mol·L^{-1}. Further bioactivity of the compounds remains to be studied.

4 CONCLUSION

Two organotin compounds tri(*o*-chlorobenzyl)tin 2,4,6-trimethylbenzoate and tri(*o*-bromobenzyl)tin salicylate have been synthesized in methanol by the microwave solvothermal method. Antitumor activity *in vitro* tests showed both compounds exhibited stronger antitumor activity against HeLa, HuH-7, A549 and H1975 than the cisplatin used in clinic.

REFERENCES

(1) Zhang, R. S.; Sun, K. X.; Zhang, S. W.; Zeng, H. M.; Zou, X. N.; Chen, R.; Gu, X. Y.; Wei, W. Q.; He, J. Report of cancer epidemiology in china 2015. *Chin. J. Ondol.* **2019**, 40, 19–28.

(2) Zaki, M.; Hairat, S.; Aazam, E. S. Scope of organometallic compounds based on transition metal-arene systems as anticancer agents: starting from the classical paradigm to targeting multiple strategies. *RSC Adv*. **2019**, 9, 3239–3278.

(3) Kenny, R. G.; Marmion, C. J. Toward multi-targeted platinum and ruthenium drugs - a new paradigm in cancer drug treatment regimens. *Chem. Rev*. **2019**, 119, 1058–1137.

(4) Vieira, F. T.; Lima, G. M.; Maia, J. R. S.; Speziali, N. L.; Ardisson, J. D.; Rodrigues, L.; Junior, A. C.; Romero, O. B. Synthesis, characterization and biocidal activity of new organotin complexes of 2-(3-oxocyclohex-1-enyl)benzoic acid. *Eur. J. Medi. Chem*. **2010**, 45, 883–889.

(5) Xiao, X.; Liang, J. G.; Xie, J. Y. Organotin(IV) carboxylates based on 2-(1,3-dioxo-1H-benzo[de]-isoquinolin-2(3H)-yl)acetic acid: syntheses, crystal structures, luminescent properties and antitumor activities. *J. Mol. Struct.* **2017**, 1146, 233–241.

(6) Yusof, E. N. M.; Latif, M. A. M.; Tahir, M. I. M.; Sakoff, J. A.; Veerakumarasivam, A.; Page, A. J.; Tiekink, E. R. T.; Ravoof, T. B. S. A. Homoleptic tin(IV) compounds containing tridentate ONS dithiocarbazate Schiff bases: synthesis, X-ray crystallography, DFT and cytotoxicity studies. *J. Mol. Struct*. **2020**, 1205, 127635–127643.

(7) He, T. F.; Zhang, F. X.; Yao, S. F.; Zhu, X. M.; Sheng, L. B.; Kuang, D. Z.; Feng, Y. L.; Yu, J. X.; Jiang. W. J. Synthesis, crystal structure and biological activities of a novel anionic organotin(IV) complex $\{[(p\text{-}ClC_6H_4CH_2)Sn(H_2O)(Cl)_2OCOCH(O)CH(O)CO_2Sn(H_2O)(Cl)_2(p\text{-}ClC_6H_4CH_2)]\cdot 2(HNEt_3)\}$. *Chin. J. Struct. Chem*. **2019**, 37, 1899–1906.

(8) Zhang, F. X.; Tao, J.; Kuang, D. Z.; Yu, J. X.; Jiang, W. J.; Zhu, X. M. Synthesis, crystal structure and properties of triphenyltin complex with salicylidene-2-aminophenol. *Chin. J. Struct. Chem*. **2019**, 38, 270–276.

(9) Attanzio, A.; D'Agostino, S.; Busà, R.; Frazzitta, A.; Rubino, S.; Girasolo, M. A.; Sabatino, P.; Tesoriere, L. Cytotoxic activity of organotin(IV) derivatives with triazolopyrimidine containing exocyclic oxygen atoms. *Molecules* **2020**, 25, 859–875.

(10) Kumari, R.; Banerjee, S.; Roy, P.; Nath, M. Organotin(IV) complexes of NSAID, ibuprofen, X-ray structure of $Ph_3Sn(IBF)$, binding and cleavage interaction with DNA and in vitro cytotoxic studies of several organotin complexes of drugs. *Appl. Organometal. Chem*. **2019**, 34, e5283–e5306.

(11) Liu, J.; Lin, Y.; Liu, M.; Wang, S.; Li, Y.; Liu, X.; Tian, L. Synthesis, structural characterization and cytotoxic activity of triorganotin 5-(salicylideneamino)salicylates. *Appl. Organometal. Chem*. **2019**, 33, e4715–e4724.

(12) Shu, S.; Zhang, F. X.; Tang, R. H.; Yan, S. Y.; Zhu, X. M.; Sheng, L. B.; Kuang, D. Z.; Yu, J. X.; Jiang, W. J. Syntheses, structures and antitumor activities of tri(*o*-bromobenzyl)tin diethyldithiocarbamate and tri(*m*-fluorobenzyl)tin pyrrolidine dithiocarbamate. *Chin. J. Struct. Chem*. **2020**, 39, 459–466.

(13) Jiang, W. J.; Kuang, D. Z.; Yu, J. X.; Feng, Y. L.; Zhang, F. X.; Wang, J. Q. Synthesis, crystal structure, quantum chemistry and thermal stability of the bis-oxygen-bridged tetranuclear dibutyltin (2,4,6-trimethyl)benzoate. *Chin. J. Inorg. Chem*. **2020**, 28, 2363–2368.

(14) Feng, Y. L.; Kuang, D. Z.; Zhang, F. X.; Yu, J. X.; Jiang, W. J.; Zhu, X. M. Two di-*n*-butyltin carboxylates with a Sn_4O_4 ladder-like framework: microwave solvothermal syntheses, structures and in vitro antitumor activities. *Chin. J. Inorg. Chem*. **2017**, 33, 830–836.

(15) Feng, Y. L.; Kuang, D. Z.; Zhang, F. X.; Yu, J. X.; Jiang, W. J.; Zhu, X. M. Microwave-solvothermal syntheses, crystal structures and in vitro antitumor activities of two bis[oxo-bis(aromatic carboxylato dibutyltin)]. *Chin. J. Inorg. Chem*. **2017**, 33, 589–594.

(16) Liu, C. L.; Xu, D.; Wen. Q.; Wang, H. X.; Xie, M. S.; Zhu, D. S. Synthesis, characterizations and thermal stability of a tricyclohexyltin carboxylate based on substituted isophthalic acid. *Chem. Bull*. **2014**, 77, 819–822.

(17) Zhang, F. X.; Kuang, D. Z.; Feng, Y. L.; Wang, J. Q.; Yu J. X.; Jiang, W. J.; Zhu, X. M. Synthesis, structure and antitumor activity of tri(*o*-bromobenzyl)tin dithiotetrahydropyrrolocarbamate. *Chin. J. Appl. Chem*. **2014**, 31, 285–289.

(18) Zhang, F. X.; He, T. F.; Yao, S. F.; Zhu, X. M.; Sheng, L. B.; Kuang, D. Z.; Yu, J. X.; Jiang, W. J. Synthesis, crystal structures and in vitro antitumor activity of two organotin hydroxybenzoate. *Chin. J. Inorg. Chem*. **2019**, 35, 598–604.